How to cite: *Angew. Chem. Int. Ed.* **2023**, *62*, e202305127
doi.org/10.1002/anie.202305127

VIP **Polymerization** *Very Important Paper*

Stochastic Simulation of Controlled Radical Polymerization Forming Dendritic Hyperbranched Polymers

Masatoshi Tosaka, Hinako Takeuchi, Masato Kibune, Tianxiang Tong, Nanyi Zhu, and Shigeru Yamago**

Abstract: Stochastic simulation of the formation process of hyperbranched polymers (HBPs) based on the reversible deactivation radical polymerization (RDRP) using a branch-inducing monomer, evolmer, has been carried out. The simulation program successfully reproduced the change of dispersities (*Đ*s) during the polymerization process. Furthermore, the simulation suggested that the observed *Đ*s (=1.5–2) are due to the distribution of the number of branches instead of undesired side reactions, and that the branch structures are well controlled. In addition, the analysis of the polymer structure reveals that the majority of HBPs have structures close to the ideal one. The simulation also suggested the slight dependence of branch density on molecular weight, which was experimentally confirmed by synthesizing HBPs with an evolmer having phenyl group.

Introduction

Highly branched polymers have attracted great deals of attention because of their unique physical properties, such as smaller hydrodynamic radius and lower intrinsic viscosity than linear counterparts. Highly branched polymers are also unique in that they have multiple chain ends that can be functionalized.[1–5] To expand the use of highly branched polymers as new materials, their structural control, i.e., the control of molecular weight and branching structure, as well as their efficient production, are important. However, conventional synthetic methods of highly branched polymers can hardly meet these requirements.[6]

Dendrimers and dendrons are the most structurally controlled highly branched polymers synthesized by stepwise coupling reaction of AC_2 monomer (A and C refer to two functional groups and 2 represents the number of C groups; the C group does not react with the A group but reacts with the A group after being converted to the B group which reacts with the A group). Due to this stepwise character, the resulting dendrimers and dendrons have defined branch structure and both dispersity and a degree of branching ($=D/(2D+L)$ where D and L are the fractions of dendritic and linear monomers, respectively[7]) being 1.0 (Figures 1a and b).[6,8–11] However, this character also makes it difficult to obtain sufficient quantities of dendrimer samples. In addition, access to dendrimers with very high branching numbers, so-called generation, has been limited because of the congestion of the reaction sites. Thus, the dendrimers and dendrons synthesized so far are usually less than the 4th generation having 124 branching points. The limit of the generation has been partly overcome by using stepwise anionic polymerization-addition reactions. For example, Hirao reported the synthesis of the 7th generation of dendritic poly(methyl methacrylate)s (PMMAs) having up to 508 branching numbers with a low *Đ* of <1.02. However, the synthesis of this dendritic PMMA required 21 steps.[8,12]

Hyperbranched polymers (HBPs, Figure 1c) are another class of highly branched polymers. They are typically synthesized in one step using polycondensation of AB_x monomer (A and B refer to two functional groups reacting with each other and x represents the number of B groups) and self-condensing vinyl (co)polymerization [SCV(C)P] using AB* monomer (A and B* refer to alkene and initiating groups, respectively).[4,12–15] Despite the simple synthetic operation, however, the structure control in HBP synthesis is usually very limited, with the degree of branching less than 1 and high *Đ* (*Đ*>4). It should be noted

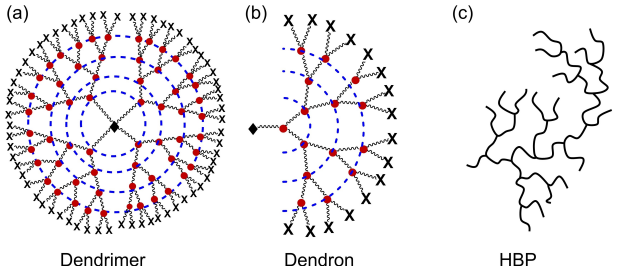

Figure 1. Schematic structures of representative highly branched polymers, a) dendrimer, b) dendron, and c) hyperbranched polymer (HBP). The structures of dendrimer and dendron correspond to the 4th generation are shown.

[*] Prof. Dr. M. Tosaka, H. Takeuchi, M. Kibune, T. Tong, N. Zhu, Prof. Dr. S. Yamago
Institute for Chemical Research, Kyoto University
Gokasho, Uji, Kyoto-fu 611-0011 (Japan)
E-mail: tosaka@scl.kyoto-u.ac.jp
yamago@scl.kyoto-u.ac.jp

that the SCV(C)P under cationic and radical polymerization conditions is a controlled polymerization condition that is effective in controlling the structure of linear polymers. However, these methods are inefficient for structural control in HBP synthesis. Some control over the HBP structure was achieved by using special polymerization conditions, such as stopping the polymerization at low monomer conversion, slow monomer addition,[16] or the use of monomer confinement under microemulsion polymerization conditions.[17] Recently, Yokozawa[18,19] and Gao[20,21] reported the controlled synthesis of HBPs by condensation polymerization using specially designed AB_2 monomer with defined reaction conditions. However, no general method has been realized so far.

In view of this problem, we have developed a novel method for the one-step synthesis of HBPs with a controlled branch structure by radical polymerization (Figure 2).[22–26] This method is based on organotellurium-mediated radical polymerization (TERP),[27,28] a type of controlled radical polymerization also called reversible deactivation radical polymerization (RDRP) using organotellurium chain transfer agent (CTA) **1**. The addition of vinyl telluride **2** induces the branching. The role of **2** is somewhat similar to the AB* monomer used in SCV(C)P, which is also called an inimer because it serves as an initiator and monomer simultaneously. However, **2** has a distinct difference from the inimer because **2** serves as the initiator only after the monomer part has reacted giving **4**. Then, stepwise activation of the two tellurium groups in **4** leads to the formation of dendritic HBP **3** through **5**. The branch efficiency was determined to be 1 by the isotope labeling experiments; therefore, the number of chain-ends could also be controlled. Hereafter, we call this comonomer an *evolmer* because **2** "evolves" its role as a monomer to that of an initiator by alternating the reactivity of the C–Te bond and enabling structural control in HBP synthesis.

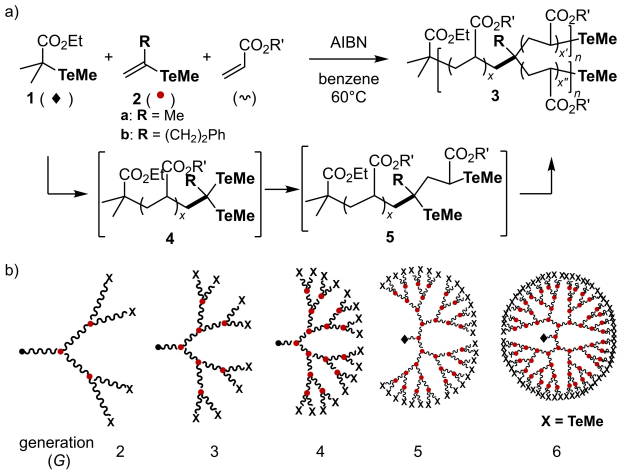

2	2a	2a	2a	2b	2b	2b
$[MA]_0/[2]_0/[1]_0$	500/3/1	500/15/1	500/63/1	960/7/1	1984/15/1	4032/31/1
generation (G)	2	4	6	3	4	5
M_n(theo) $\times 10^{-4}$	4.12	3.96	3.46	7.78	15.93	32.18
M_n(SEC) $\times 10^{-4}$	4.21	2.56	0.98	4.85	9.42	17.28
M_n(MALS) $\times 10^{-4}$	5.37	5.73	5.39	8.29	17.14	37.84
$Đ$	1.55	1.71	1.99	1.88	1.97	2.09

Figure 2. One-step synthesis of structurally controlled HBPs by TERP using evolmer **2**. a) Reaction Scheme and b) schematic structure of the obtained HBPs and summary of polymerization results, in which the ones using **2a** have been reported in our previous work,[22] while the others using **2b** were newly synthesized for the current work. MA denotes methyl acrylate. $Đ$ was calculated based on the signals of the refractive index detector. M_n(MALS) was obtained by dividing M_w-(MALS) by $Đ$, in which M_w(MALS refers to the weight-average molecular weight determined by MALS.

One of the most striking features of this method is the possible control of the dendritic generation (G) by changing the ratio of **1** and **2** (Figure 2b). Indeed, our previous experimental results showed that the number-averaged molecular weight determined by size exclusion chromatography (SEC, $M_{n(SEC)}$) became smaller as the increase of the $[\mathbf{2}]_0/[\mathbf{1}]_0$ ratio. In contrast, the absolute molecular weights determined by multi-angle laser light scattering (MALS, $M_{n(MALS)}$) were very close to those of theoretical values ($M_{n(theo)}$) (see the table in Figure 2b). The results are consistent with the fact that the hydrodynamic volumes of polymers decrease with increased branching. However, the $Đ$s of the resulting HBPs were usually between 1.5 and 2. These values were significantly improved from the conventional HBP synthesis by radical polymerization using SCV(C)P. However, they were still higher than those usually observed for the synthesis of linear polymer using RDRP. Also, the $Đ$s were significantly higher than the dendritic PMMA synthesized by the anionic polymerization/coupling reaction.[6,8]

The same strategy for the structure control of HBPs based on atom transfer radical polymerization (ATRP) and reversible addition-fragmentation-chain transfer (RAFT) conditions was also reported by Zhong[29] and Chen,[30] in which α-bromoacrylate and 1-bromo-1-trifluoromethylethene were used as an evolmer, respectively. Very recently, the application of the ATRP method in water using α-bromoacrylic acid as an evolmer was reported by Matyjaszewski.[31] The characteristic features of these reports are low $Đ$s ($Đ < 1.5$), and the results contradicted our results. It should be noted that the $Đ$s of HBPs, recently reported by Zhong using ATRP, were higher ($Đ = 1.5$–2.0) than their initial report when the conversion of the evolmer was high.[32] These differences in $Đ$s raised a question; what would be the values of $Đ$ of HBPs synthesized by this strategy without any undesirable side reactions, i.e., termination reactions.

To confirm the optimum $Đ$s of the HBPs synthesized by this strategy, we carried out stochastic computer simulations on the formation process of HBPs by TERP. While the increased $Đ$ was possibly occurred by the increased termination reaction due to the proximity effect of the dormant ends, as pointed by Zhong,[32] the results clearly indicate that the increase in the $Đ$ is not due to the termination reaction. Instead, the increase of $Đ$ originates from the distribution of the number of branches. Furthermore, the simulation indicates the branched structures of the HBPs are well-controlled. These results, combined with the resemblance of the simulation and our experimental results, strongly sup-

port the successful synthesis of structurally controlled HBPs with dendritic structure by the TERP method.

Results and Discussion

The stochastic simulation program was created based on the reaction kinetics of the elementary steps of the current HBP synthesis based on TERP (See Supporting Information for details). The polymerization mechanism of TERP is the degenerative chain transfer.[12,18] Therefore, the current HBP synthesis consists of three elementary steps, i.e., propagation of polymer end radical $P^\bullet$ to monomer M, cross propagation of $P^\bullet$ to evolmer E, and chain transfer between $P^\bullet$ and dormant species PX (polymer chain end or CTA) with the rate constants k_p, k_b, and k_{ex}, respectively (Figure 3). In addition, the undesired termination reaction between two radicals $P^\bullet$ and $P'^\bullet$ also takes place with the rate constant k_t.

An elementary reaction that an active radical species will take is stochastically determined as one of those in Figure 3 based on their relative reaction rates. The corresponding elementary reaction rates are formulated as in Figure 4.

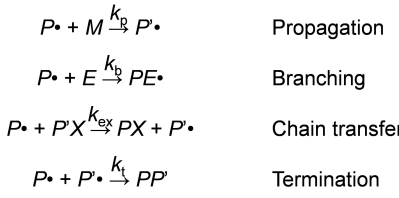

Figure 3. Elementary reactions in the current HBP synthetic method.

$$v_p = k_p[P\cdot][M] \quad \left(= -\frac{d[M]}{dt}\right)$$

$$v_b = k_b[P\cdot][E] \quad \left(= -\frac{d[E]}{dt}\right)$$

$$v_{ex} = k_{ex}[P\cdot][PX]$$

$$v_t = k_t[P\cdot]^2 \quad \left(= -\frac{1}{2}\frac{d[P\cdot]}{dt}\right)$$

Figure 4. Rates of elementary reactions in the current HBP synthetic method; v_p, v_b, v_{ex}, v_t are reaction rate of propagation, branching, chain transfer and termination, respectively, and t is time.

$$P_p = \frac{v_p}{v_p + v_b + v_{ex} + v_t} = \frac{k_p[M]}{k_p[M] + k_b[E] + k_{ex}[PX] + k_t[P\cdot]}$$

$$P_b = \frac{v_b}{v_p + v_b + v_{ex} + v_t} = \frac{k_b[E]}{k_p[M] + k_b[E] + k_{ex}[PX] + k_t[P\cdot]}$$

$$P_{ex} = \frac{v_{ex}}{v_p + v_b + v_{ex} + v_t} = \frac{k_{ex}[PX]}{k_p[M] + k_b[E] + k_{ex}[PX] + k_t[P\cdot]}$$

$$P_t = \frac{v_t}{v_p + v_b + v_{ex} + v_t} = \frac{k_t[P\cdot]}{k_p[M] + k_b[E] + k_{ex}[PX] + k_t[P\cdot]}$$

Figure 5. Probability of selection of elementary reactions in the current HBP synthetic method. P_p, P_b, P_{ex}, and P_t are the probability of taking propagation, branching, chain transfer and termination, respectively.

As a selection of one of these elementary reactions results from competition among them, the probability of selection of each elementary step is written as equations in Figure 5 with $P_p + P_b + P_{ex} + P_t = 1$, when no other reaction occurs.

Based on these equations and considering the changes in the number of chemical species, the formation of HBPs starting from 10000 molecules of CTA was simulated. ($[PX]_0 = 10000$; see Supporting Information for details. The square bracket usually indicates molar concentration. In the simulation program, however, we can regard it as the number of the chemical species indicated in it.) The $Đ$s were calculated for the 10000 polymers formed.

The validity of the program was examined by the reproducibility of $Đ$s. Prior to HBPs, polymerization of methyl acrylate (MA) giving linear polyMA (PMA) was simulated by taking $k_p = 2.40 \times 10^4\ \mathrm{mol\,L^{-1}\,s^{-1}}$ and $k_{ex} = 4.60 \times 10^5\ \mathrm{mol\,L^{-1}\,s^{-1}}$, values at 60 °C from the literature.[27] The effect of the termination was not considered at first ($k_t = 0$) for the sake of simplicity. The simulation with $[M]_0/[E]_0/[PX]_0 = 500/0/1$ showed that $Đ$s decreased with monomer conversion and finally reached 1.05 (Figure 6a, Y = 0). This result was virtually identical to the previous simulation based on the analytical prediction[33] (See Supporting Information for details).

Next, the $Đ$s for HBP were simulated. The k_p and k_{ex} of $P^\bullet$ derived from MA and **2a** can be different, but they were assumed to be equal for simplicity. As the k_b has not been known, it was estimated to be $4.23 \times 10^3\ \mathrm{mol\,L^{-1}\,s^{-1}}$ based on the copolymerization kinetics in our previous work.[22] The effect of the termination was also unconsidered here ($k_t = 0$).

Figure 6a shows the simulation results for HBPs with $[M]_0/[E]_0/[PX]_0 = 500/\mathrm{Y}/1$ (Y = 3, 7, 15, 31, and 63), which correspond to our previous experimental work for the synthesis of 2nd to 6th generation of HBPs (runs 1–5 of Table 1 in Ref. [22]). The $Đ$s quickly decrease and reach to plateau in all cases. For example, the $Đ$ value becomes constant before 10 % monomer conversion for the simulation results for Y = 63, and the results are consistent with the experimental data (Figure 6b). The monomer conversion to reach the plateau depends on Y and is less for the higher amount of Y. For example, for Y = 3, about 40 % monomer consumption is required to reach the plateau, but Y = 63 needs about 10 %. The final $Đ$s at 100 % monomer conversion are also Y dependent and increase with the increase of Y (Figure 6a). For example, the final $Đ$ for Y = 3 is 1.60, and that for Y = 63 is 2.00, and these values agree well with the experimental results (1.62 and 1.99, respectively. See Figure 6c).[22] The excellent reproducibility of the experimental results clearly validates the current simulation.

The simulation was also carried out for the previous HBP syntheses by changing $[M]_0/[E]_0/[PX]_0$ ratios shown in runs 7–10 of Table 1 in Ref. [22]. The correlation of all experimental and simulated final $Đ$s was in good agreement with the correlation coefficient of 0.84 (Figure 6c), further validating the current simulation. There is one point showing

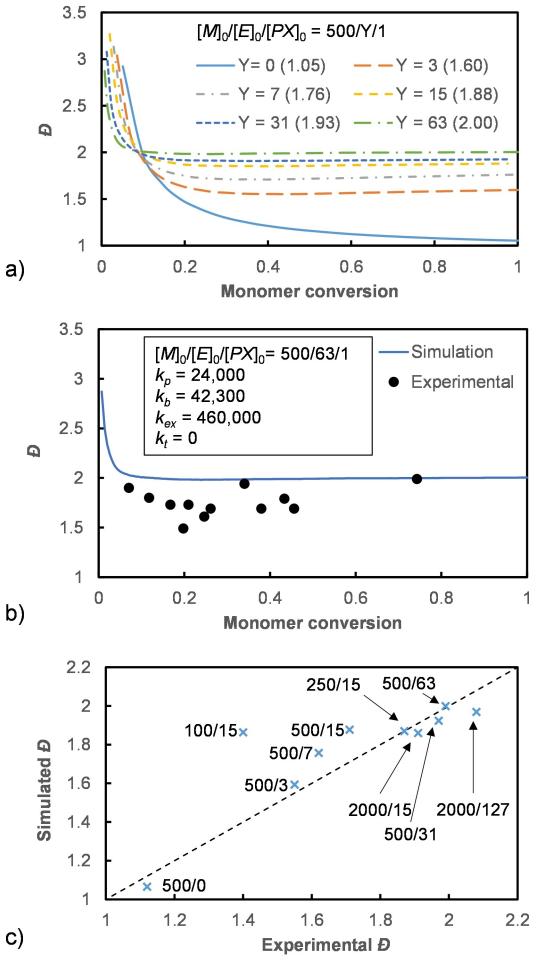

Figure 6. a) Simulated dependence of $Đ$ on monomer conversion for linear and HBPs. Values in the parenthesis in the legend indicate the final value of $Đ$. $[PX]_0 = 10000$. The condition corresponds to runs 1–6 of Table 1 in Ref. [22]. b) Simulated and experimental dependence of $Đ$ for hyper-branched polymer. The condition corresponds to run 5 of Table 1 in Ref. [22]. c) Comparison between simulated and experimental $Đ$s, assuming the absence of termination reaction. Experimental data were taken from runs 1–10 of Table 1 in Ref. [22]; $[M]_0/[E]_0/[PX]_0 = 500/3/1$, 500/7/1, 500/15/1, 500/31/1, 500/63/1, 500/0/1, 100/15/1, 250/15/1, 2000/15/1 and 2000/127/1. Values of $[M]_0/[E]_0$ are indicated in the Figure.

significantly higher experimental $Đ$ compared to that of the simulation ($[M]_0/[E]_0/[PX]_0 = 100/15/1$), but this is probably due to the short targeted segment length between branch points (≈ 3 MA units). Steric hindrance near the branch points probably prevented the regular growth of each chain.

While the $[E]_0/[PX]_0$ ratio, Y, significantly affects the final $Đ$s (Figure 6a), the $[M]_0/[PX]_0$ ratio, Z, has only a negligible effect. For example, the results by varying Z = 100–2000 with keeping the same $[E]_0/[PX]_0 = 15$ are shown in Figure 7. The decrease of $Đ$s as the increase of monomer conversion was slightly different, but the final $Đ$ values are identical at all. The same simulation results were also obtained for Z = 3, 7, 31, and 63 (Figure S6).

The simulation demonstrated that final $Đ$s are more than 1.5 in all cases for HBPs with Y > 3, strongly suggesting that

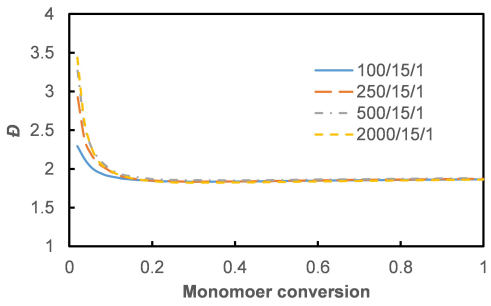

Figure 7. Simulated dependence of $Đ$ on monomer conversion for branched polymers, assuming the absence of termination reaction. $[PX]_0 = 10000$. The conditions correspond to runs 3, 7–9 of Table 1 in Ref. [22].

the high $Đ$ values in our HBP synthesis are not due to the termination reaction but an inherent issue for the HBP formation process, as discussed below. Indeed, the simulation including the termination reactions resulted in significantly higher $Đ$s than the experimental values (See Supporting Information).

The most significant advantage of this stochastic simulation is the access to detailed structural information of each HBP molecule generated by the simulation. Therefore, the validity of the proposed structures shown in Figure 2b was examined by the weight and the number distribution of the HBPs against the degree of polymerization (DP) and the number of evolmers (N_{EV}) incorporated into the HBP.

Figure 8 shows the distribution of the HBPs against DP and the number of the evolmer for Y = 63. The weight distribution, which usually determines the physical properties of polymers, indicates that the most abundant HBP has

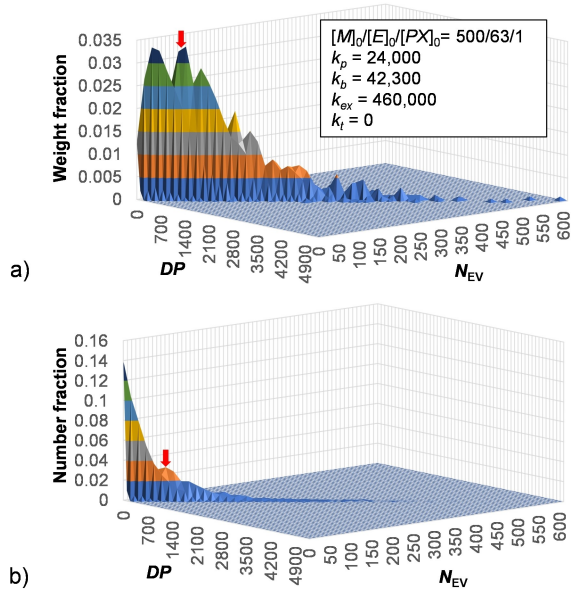

Figure 8. Number (a) and weight (b) distribution of simulated structure of HBP. $[PX]_0 = 10000$. The condition corresponds to run 5 of Table 1 in Ref. [22]. The intended structure is indicated by the arrow in the right part.

a DP of 564, which agrees with the theoretical DP of 564 (Figure 8a, see also Figure S7). The formation of a small amount (<0.5 %) of very high molecular weight HBPs with DPs over 3000 and a significant amount of low molecular weight polymers was also observed. Therefore, the formation of such high and low molecular weight HBPs is the origin of the high $Đ$ of HBPs.

However, the presence of high and low molecular weight HBPs does not mean the loss of control of the branched structure, as indicated by an excellent good correlation between DP and the N_{EV}s in it (Figure 8 and S7). The previous theoretical prediction indicates the activation efficiencies of the dormant species **4** and **5** are very similar.[22,25] Furthermore, the branch efficiency experimentally obtained is almost 100 %.[22,25] Therefore, the observed periodical insertion of the evolmer implies the successful control of the branch structure.

The same structural analysis of the HBPs simulated under different $[M]_0/[E]_0/[PX]_0$ ratios also shows that the significant weight distribution of the ideal structure in all cases, especially $[E]_0/[PX]_0$ ratios more than 7 (Figure S8). The results strongly imply control of the "generation" of our HBPs, as already reported for dendrimers and dendrons.

The number distribution, on the other hand, indicates that many HBPs tend to remain low DP because of the formation of very high molecular weight HBPs. Nevertheless, the distribution still has the apex at the ideal structure (indicated by the arrow in Figure 8b). In actual experiments, the fraction with the small DP can be removed by the purification process, e.g., reprecipitation.

Figure 8 also implies that the number of dormant ends increases with increasing DP and molecular weight due to the insertion of evolmers. The situation sharply contrasts linear polymer formation, in which one polymer always has only one dormant end. As the reactivity of the dormant ends must be very similar regardless of the branched structure, the molecular weight increases further in proportion to the number of dormant ends. Therefore, the distribution of the number of branches is the reason for the higher $Đ$ values of HBPs than linear polymers.

The above discussion also suggests a decrease in $Đ$s with the decrease in branch efficiency. This view is supported by the effect of Y on the $Đ$s, as shown in Figure 6a, because the evolmers that do not act as branch points can be regarded as conventional monomers. Therefore, low $Đ$s observed in other works[14–6] are most likely due to the low branch efficiency.

Finally, the uniformity of *segments* in an HBP, defined as linear units between adjacent branch points or between the outermost branch point and the chain ends, was investigated in more detail by this simulation. Thus, the structure of HBPs with the same theoretical segment length (64 monomer units) but different generations and DPs was simulated with the initial parameters $[M]_0/[E]_0/[PX]_0$=Z/Y/1 (Z/Y= 960/7, 1984/15, and 4032/31, correspond to 3rd, 4th, and 5th dendritic generation, respectively).

Surprisingly, the simulation indicated the presence of a gradient of the average segment length, which decreases as increasing N_S, the number of branching points from the initiating point to the segment in question (Figure 9a). Namely, the segment length is longer than the theoretical value near the initiating point (≈80 monomer units) but gradually becomes shorter as N_S increases. Furthermore, the observed dependence is most pronounced for the HBPs of the lowest generation (the 3rd generation) followed by the 4th generation, and then, the 5th generation.

Due to the presence of the gradient, the average branch density defined by the ratio of the branch point in an HBP (N_{EV}/DP) is also DP dependent (Figure 9b). The average branch density is particularly lower than the ideal values ($\approx 7.5\times10^{-3}$) for the HBPs with the DP of less than 1000. Since the HBP simulated with Z/Y=960/7 has the highest weight fraction at the DP of ≈1000, certain levels of contribution from HBPs with longer segment lengths than the ideal length appear to be present. However, the highest weight fractions of the HBPs simulated with Z/Y=1984/15, and 4032/31 are sufficiently higher than the DP of ≈1000, the effect of the gradient are virtually negligible and the HBPs with average branch density close to the ideal values are predominantly formed.

The results in Figure 9 were tested experimentally by synthesizing HBPs using new evolmer **2b** (Figure 2, R=$(CH_2)_2$Ph), which has a phenyl group. Since **2b** has a phenyl group, the amount of evolmer incorporated into the HBPs can be quantified as a function of molecular weight by SEC-MALLS analysis equipped with ultraviolet (UV), refractive index (RI), and MALS detectors. Namely, the intensity of the signal detected by the RI detector (I_{RI}) is proportional

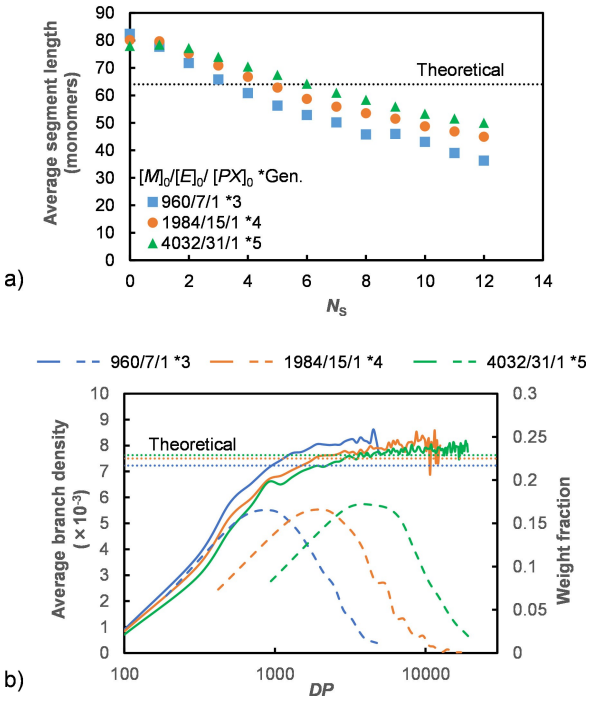

Figure 9. Relationship between a) N_S and average segment length, and b) DP and average branching density (solid line) along with the weight distribution of HBPs (broken line), obtained by the simulation. The dendritic generation of the sample is indicated after the asterisk in the legend. Horizontal dotted lines indicate the theoretical values.

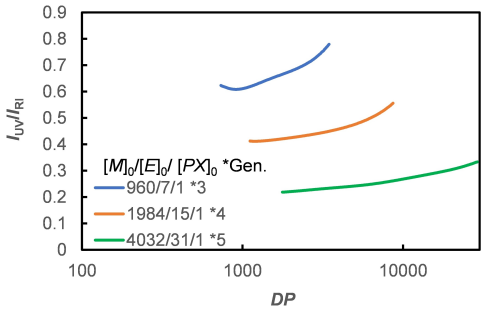

Figure 10. Experimentally obtained relationship between *DP* and I_{UV}/I_{RI} for HBP samples using **2b**.

to only the concentration of HBPs, but that by the UV detector (I_{UV}) is proportional to both the concentration and the branch number. Therefore, relative change of the branch density was evaluated by the I_{UV}/I_{RI} as the function of the absolute molecular weight or *DP* determined by the MALS detector.

The HBP syntheses were carried out under the same conditions used for the simulation ($[MA]_0/[\mathbf{2b}]_0/[\mathbf{1}]_0 = Z/Y/1$ with Z/Y = 960/7, 1984/15, and 4032/31) at 60 °C. Copolymerization of **2b** and MA took place statistically with a similar reactivity ratio as in the case of **2a** and both monomers reached nearly quantitative conversion (> 99 % for **2b** and > 85 % for MA). Furthermore, the resulting HBPs showed the characteristic SEC results, in which $M_{n(SEC)}$s were significantly smaller than theoretical M_n ($M_{n(theo)}$) but $M_{n(MALS)}$s were very similar to $M_{n(theo)}$. The SEC traces were unimodal in all cases, and *Đ*s were 1.88–2.09 (See Supporting Information for details).

The SEC-MALS results showed the increase of branch density with *DP* (Figure 10), namely, the segment length gradually decreases as the increase of the number of segments. Furthermore, the effect of the I_{UV}/I_{RI} on *DP* was more pronounced for smaller X/Y. These results are consistent with the trend obtained by the simulation. Further studies including the optimization of the simulation conditions would be necessary to have more quantitative and accurate results.

Conclusion

The stochastic simulation of the formation process of HBPs based on the RDRP using an evolmer was performed. The simulation results suggested that the higher *Đ*s of HBPs than linear counterparts arise from the distribution of the number of branches instead of undesired side reactions, such as the termination reaction. Furthermore, the majority of HBPs have structures close to the ideal one, and accordingly, the structure is successfully controlled. The insights about the structures of HBPs gained from the simulations are verified experimentally.

Supporting Information

Supporting information for this article is available on the WWW under https://doi.org/10.1002/anie.202305127. The authors have cited additional references within the Supporting Information.

Acknowledgements

This work was supported by JSPS KAKENHI Grant Numbers 21H05027 (S.Y.) and 21K05184 (M.T.).

Conflict of Interest

The authors declare no conflict of interest.

Data Availability Statement

The data that support the findings of this study are available in the Supporting Information of this article.

Keywords: Dendrimer · Hyperbranched Polymer · Polymerization Kinetics · Reversible-Deactivation Radical Polymerization · Simulation

[1] B. I. Voit, A. Lederer, *Chem. Rev.* **2009**, *109*, 5924–5973.
[2] C. Gao, D. Yan, *Prog. Polym. Sci.* **2004**, *29*, 183–275.
[3] M. Jikei, M. Kakimoto, *Prog. Polym. Sci.* **2001**, *26*, 1233–1285.
[4] *Hyperbranched Polymers: Synthesis, Properties, and Applications* (Eds.: D. Yan, C. Gao, H. Frey), Wiley, Hoboken, **2011**.
[5] N. Hadjichristidis, M. Pitsikalis, S. Pispas, H. Iatrou, *Chem. Rev.* **2001**, *101*, 3747–3792.
[6] G. Polymeropoulos, G. Zapsas, K. Ntetsikas, P. Bilalis, Y. Gnanou, N. Hadjichristidis, *Macromolecules* **2017**, *50*, 1253–1290.
[7] A. Fradet, J. Chen, K. H. Hellwich, K. Horie, J. Kahovec, W. Mormann, R. F. T. Stepto, J. Vohlídal, E. S. Wilks, *Pure Appl. Chem.* **2019**, *91*, 523–561.
[8] A. Hirao, R. Goseki, T. Ishizone, *Macromolecules* **2014**, *47*, 1883–1905.
[9] S. M. Grayson, J. M. J. Fréchet, *Chem. Rev.* **2001**, *101*, 3819–3868.
[10] D. A. Tomalia, J. B. Christensen, U. Boas, *Dendrimers, Dendrons, and Dendritic Polymers: Discovery, Applications, and the Future*, Cambridge University Press, Cambridge, **2012**.
[11] A. W. Bosman, H. M. Janssen, E. W. Meijer, *Chem. Rev.* **1999**, *99*, 1665–1688.
[12] P. J. Flory, *J. Am. Chem. Soc.* **1952**, *74*, 2718–2723.
[13] J. M. J. Fréchet, M. Henmi, I. Gitsov, S. Aoshima, M. R. Leduc, R. B. Grubbs, *Science* **1995**, *269*, 1080–1083.
[14] P. J. Flory, *Principles of Polymer Chemistry*, Cornell University Press, New York, **1953**.
[15] Y. H. Kim, O. W. Webster, *J. Am. Chem. Soc.* **2002**, *124*, 4592–4593.
[16] R. Hanselmann, D. Hölter, H. Frey, *Macromolecules* **1998**, *31*, 3790–3801.
[17] K. Min, H. Gao, *J. Am. Chem. Soc.* **2012**, *134*, 15680–15683.
[18] Y. Ohta, S. Fujii, A. Yokoyama, T. Furuyama, M. Uchiyama, T. Yokozawa, *Angew. Chem. Int. Ed.* **2009**, *48*, 5942–5945.

[19] Y. Ohta, K. Sakurai, J. Matsuda, T. Yokozawa, *Polymer* **2016**, *101*, 305–310.
[20] Y. Shi, R. W. Graff, X. Cao, X. Wang, H. Gao, *Angew. Chem. Int. Ed.* **2015**, *54*, 7631–7635.
[21] X. Cao, Y. Shi, H. Gao, *Synlett* **2017**, *28*, 391–396.
[22] Y. Lu, T. Nemoto, M. Tosaka, S. Yamago, *Nat. Commun.* **2017**, *8*, 1863.
[23] Y. Lu, S. Yamago, *Angew. Chem. Int. Ed.* **2019**, *58*, 3952–3956.
[24] Y. Lu, S. Yamago, *Macromolecules* **2020**, *53*, 3209–3216.
[25] S. Yamago, *Polym. J.* **2021**, *53*, 847–864.
[26] Y. Jiang, M. Kibune, M. Tosaka, S. Yamago, *ChemRxiv*. **2023**, https://doi.org/10.26434/chemrxiv-2023-63gsc.
[27] S. Yamago, *Chem. Rev.* **2009**, *109*, 5051–5068.
[28] S. Yamago, K. Iida, J. Yoshida, *J. Am. Chem. Soc.* **2002**, *124*, 2874–2875.
[29] F. Li, M. Cao, Y. Feng, R. Liang, X. Fu, M. Zhong, *J. Am. Chem. Soc.* **2019**, *141*, 794–799.
[30] Y. Zhao, M. Ma, X. Lin, M. Chen, *Angew. Chem. Int. Ed.* **2020**, *59*, 21470–21474.
[31] K. Kapil, G. Szczepaniak, M. R. Martinez, H. Murata, A. M. Jazani, J. Jeong, S. R. Das, K. Matyjaszewski, *Angew. Chem. Int. Ed.* **2023**, *62*, e202217658.
[32] M. Cao, Y. Liu, X. Zhang, F. Li, M. Zhong, *Chem* **2022**, *8*, 1460–1475.
[33] T. Fukuda, A. Goto, Y. Tujii, *Handbook of Radical Polymerization* (Eds.: K. Matyjaszewski, T. P. Davis), Wiley-Interscience, New York, **2002**, pp. 407–462.

Manuscript received: April 12, 2023
Accepted manuscript online: May 17, 2023
Version of record online: June 14, 2023